

Report No. UT-00.13

***STATIC AND DYNAMIC
TESTING OF A CURVED,
STEEL GIRDER BRIDGE IN
SALT LAKE CITY, UTAH***

FINAL REPORT

**By: Kevin Womack, Ph.D., P.E.
Marvin Halling, Ph.D., P.E.
Stephen Bott**

**Department of Civil &
Environmental Engineering
Utah State University**

**Utah Department of Transportation
Research Division**

August 2001

UDOT RESEARCH & DEVELOPMENT REPORT ABSTRACT

1. Report No. UT-00.13		2. Government Accession No.		3. Recipient's Catalog No.	
4. Title and Subtitle Static and Dynamic Testing of a Curved, Steel Girder Bridge in Salt Lake City, Utah		5. Report Date August 2001			
		6. Performing Organization Code			
7. Author(s) Womack, Kevin Halling, Marvin		8. Performing Organization Report No. UT-00.13			
9. Performing Organization Name and Address Department of Civil and Environmental Engineering Utah State University Logan, Utah 84322-4110		10. Work Unit No.			
		11. Contract No.			
12. Sponsoring Agency Name and Address Utah Department of Transportation Research Division 4501 South 2700 West Salt Lake City, Utah		13. Type of Report and Period Covered Final Report, May 1999 to August 2001			
		14. Sponsoring Agency Code			
15. Supplementary Notes					
16. Abstract <p>A three span, curved steel girder bridge, 152 feet in length, slated for demolition in the Fall of 1999 was tested both statically and dynamically under three different boundary conditions. The objective of these tests were to 1) collect data on the behavior of curved steel girders under load, 2) investigate the ability of modal analysis to determine changes in boundary conditions (or structural damage), and 3) to provide field test data for the verification of a finite element model.</p> <p>The testing of the bridge was successfully completed in the Summer of 1999. Since that time a detailed finite element model of the bridge, using plate elements, has been constructed using SAP2000. The data from the tests has been reduced and influence diagrams for both the static test and the finite element model have been produced, and show a good match between model and field tests. The dynamic test data has been analyzed and shows an ability to detect the changes in the boundary conditions via the change in natural frequencies and mode shapes.</p>					
17. Key Words System identification, modal analysis, natural frequencies, mode shapes, non-destructive evaluation, forced vibration, load testing, curved girder, influence lines.		18. Distribution Statement Available: UDOT Research Division Box 148410 Salt Lake City, Utah 84114-8410 www.udot.utah.gov/res			
19. Security Classification (of this report) N/A	20. Security Classification (of this page) N/A	21. No. of Pages 37		22. Price N/A	

Abstract

A three span, curved steel girder bridge, 152 feet in length, slated for demolition in the Fall of 1999 was tested both statically and dynamically under three different boundary conditions. The objectives of these tests were to 1) collect data on the behavior of curved steel girders under load, 2) investigate the ability of modal analysis to determine changes in boundary conditions (or structural damage), and, 3) to provide field test data for the verification of a finite element model.

The testing of the bridge was successfully completed in the Summer of 1999. Since that time a detailed finite element model of the bridge, using plate elements, has been constructed using SAP2000. The data from the tests has been reduced and influence diagrams for both the static test and the finite element model have been produced, and show a good match between model and field tests. The dynamic test data has been analyzed and shows an ability to detect the changes in the boundary conditions via the change in natural frequencies and mode shapes.

Acknowledgements

We would like to express our appreciation to all those who made this research possible and assisted in the field testing: Hamid Ghasemi, Sheila Duwadi, Joey Hartman and James D. Cooper of the Federal Highway Administration; Sam Sherman of the Utah Department of Transportation; Jeff Schultz and his crew at Bridge Diagnostics, Inc.; Emin Aktan of Drexel University; and our graduate students who contributed mightily to the testing and data analysis.

Much of the material for this report was taken from the report supplied by Bridge Diagnostics, Inc. (BDI) as part of their subcontract. The BDI report will not be called out as a reference within this report. Any person desiring a copy of the BDI report should contact one of the authors of this report.

Contents

Introduction	1
Test Bridge.....	2
Testing	3
Static Testing	8
Static Loading	8
Instrumentation.....	8
Static Testing Procedure	14
Dynamic Testing	15
Dynamic Loading.....	16
Instrumentation.....	17
Dynamic Testing Procedure	17
Computer Model.....	18
Results	20
Crawl Load Tests	20
Phase 1 Tests	20
Phase 2 Tests	25
Phase 3 Tests	27
Static Load Tests	27
Computer Model.....	27
Dynamic Testing	28
Conclusions.....	32
Static Testing	32
Computer Model.....	33
Dynamic Testing	34

Static and Dynamic Testing of a Curved Steel Girder Bridge in Salt Lake City, Utah

Kevin C. Womack, Associate Professor

Dept. of Civil and Environmental Engineering, Utah State University
Logan, Utah

Marvin W. Halling, Associate Professor

Dept. of Civil and Environmental Engineering, Utah State University
Logan, Utah

Stephen P. Bott

ARW Engineers
Ogden, Utah

Introduction

The reconstruction of the Interstate 15 (I-15) freeway through Salt Lake City, Utah has provided many opportunities for the destructive testing of bridges that have been slated for demolition. Nearly \$2 million has been provided by the Federal Highway Administration (FHWA) for structural and geotechnical research on the I-15 corridor during its reconstruction.

A current research priority of FHWA engineers at the Turner-Fairbanks research facility in McLean, Virginia is the behavior of curved steel girders. Upon discovery that a curved steel girder bridge on the I-15 corridor was slated for demolition in the Fall of 1999 it was decided that this bridge should be tested. The testing of the bridge in Salt Lake City will go as a companion project to the full scale curved steel girder tests that are currently being conducting at the Turner-Fairbanks facility.

The primary objective for testing the bridge in Salt Lake City is to provide data on the behavior of a specific curved steel girder bridge that can be used to validate a computer model of that bridge. A secondary objective is to examine the potential for using dynamic testing as a non-destructive evaluation technique. The scope of this report is to present the static test data compared with the output of the computer model and the results of the dynamic testing. The results of the static testing and computer modeling is presented primarily through the use of influence diagrams contained on the enclosed CD.

In the soon to begin second phase of this research the test data and the computer model will be used to perform a comparison of the types of analyses that can be performed to predict the behavior of curved girders. These analyses

will range from simple straight beam analyses to very complicated computer analyses. It is anticipated that a minimal level of analysis that provides a reasonable prediction of curved girder will be determined.

Eventually the data from the tests conducted on the bridge in Salt Lake City, the computer model developed as a result of these tests, and the data compiled from the curved girder tests being conducted at Turner-Fairbanks will be used in the development of Load Resistance Factor Design (LRFD) design equations for curved steel girders.

Test Bridge

The curved bridge tested on the 1-15 corridor in Salt Lake City was built in the early 1970's and was located at the southern interchange of 1-15 and 1-215, it carried northbound traffic from 1-15 to the westbound lanes of 1-215. This bridge, the second bridge seen in Figure 1, was out of commission for almost a year before demolition and was replaced by a much longer bridge (foremost bridge in Figure 1).



Figure 1. Northbound 1-15 Ramps to Westbound 1-215

The test bridge, designated as Ramp A-6, was a curved, continuous three span, welded plate girder bridge. The span lengths along the survey line were 12.6 m (41 ft 6 in) for the outside spans and 21.1 m (69 ft 3 in) for the center span. The radius of curvature to the survey line of the bridge was 145.6 m (478

ft), see Figure 2. The alignment of the bridge followed a vertical curve which transitioned from a slope of -1.47% at the south end of the bridge to -6.06% over a distance of 106.7 m (350 ft) to the north. The deck also had a super-elevation of 6% (see Figures 3, 4). The width of the bridge was 12.9 m (42 ft 4 in) to the outside of the parapets with an actual deck width of 11.7 m (38 ft 6 in).

Five girders supported the bridge deck, spaced at 2.7 m (8 ft 10 in) on centers (see Figures 3, 5). The first three girders on the left side of the elevation shown in Figure 3 (numbered 1, 2 and 3) were identical in cross section. The right two girders (4 and 5) were identical with heavier flanges (see Table 1). All five girders had an increase in flange thickness 9.14 (30 ft) from each abutment.

Web stiffeners were placed only one side of each girder, the inside of the curve, except for Girder 1 where the stiffeners were placed on the outside curve. These stiffeners were typically spaced at 0.92 m (3 ft). Diaphragms were placed radially between the girders and spaced at 4.62 m (13 ft 10 in) along the center line of the bridge. These diaphragms were C15 X 40 sections.

The bridge deck consisted of a 216 mm (8.5 in) thick reinforced concrete slab topped by 76 mm (3 in) of asphalt. The concrete slab was integral with the abutment, including continuous reinforcement. Based on compression tests of cores cut from the deck the concrete had a strength of 35.1 MPa (5100 psi). The deck and the steel support girders acted in a non-composite manner. This was evident from visual inspection of the bridge that there had been obvious differential movement between the deck and the girders, this was also evident from the results of the tests that were run.

The overall condition of the bridge deck and steel support girders was very good, with no decay of the concrete on the underside of the deck and very little corrosion of the steel girders (see Figure 6).

The supports for the bridge on both the abutments and piers were self-lubricating bronze bearings. From visual inspection it appeared that the bearings on the abutments were no longer functional in terms of allowing the bridge to move longitudinally, the bridge had shifted and damaged the bearings. Just prior to the third phase of testing it was discovered that three of the supports on the piers had been welded which did not allow the bearings to rock.

Testing

Three testing phases were conducted. The first phase was with the bridge in an as-is condition. The second and third phase tests were conducted with changes in the boundary conditions. In order to investigate the dynamic testing as a method of non-destructive method for detecting structural damage the bridge had to be "damaged" in some way after the first phase of testing. Due to the fact that the bridge crossed over an active Interstate freeway with live traffic

Web Thickness	8.69 mm (0.342 in)
Flange Thickness Girders 1 – 3, thin section	19.6 mm (0.773 in)
Flange Thickness Girders 1-3, thick section	36.1 mm (1.42 in)
Flange Thickness Girders 4-5, thin section	26.4 mm (1.04 in)
Flange Thickness Girders 4-5, thick section	43. mm (1.69 in)
Bearing Stiffeners, end supports	152.4 mm x 12.7 mm (6 in x ½ in) Plate
Bearing Stiffeners, interior supports	152.4 mm x 28.6 mm (6 in x 1 1/8 in) Plate
Diaphragm Stiffeners	114.3 mm x 7.94 mm (4 ½ in x 5/16 in) Plate
Diaphragm Connection Plates	152.4 mm x 9.53 mm (6 in x 3/8 in) Plate
Intermediate Diaphragms	C 15 x 40 Standard Section

Table 1. Dimensions of Plate Girder Components

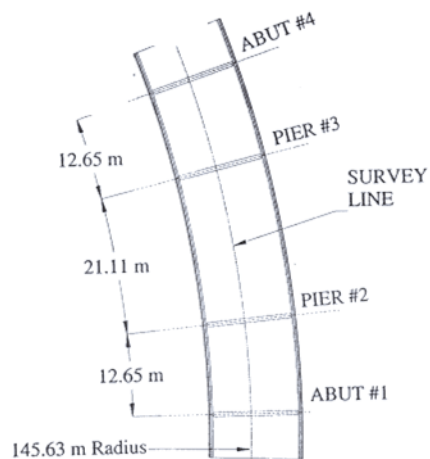


Figure 2. Plan View of Bridge

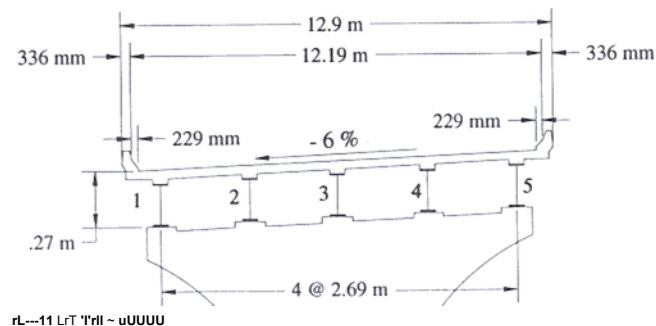


Figure 3. Elevation of Pier (looking North)



Figure 4. View of Bridge Deck -Looking North



Figure 5. View of Bridge Underside -Looking North



Figure 6. Close-up View of Bridge Underside

the bridge could not be damaged, so the boundary conditions at the abutments were changed; significantly, but not in a way that would place in doubt the integrity of the structure. Again, this was done to accommodate the dynamic testing, but it also provided the opportunity to test a "different" curved girder structure statically as well.

For the second phase of the testing the integral deck and abutment were separated by cutting the deck (see Figure 7). The intent was to "free" up the end boundary conditions. The change in boundary conditions for the third phase of testing consisted of jacking up the support girders at the abutments, taking the girder ends off of the bronze bearings and placing them on frictionless stainless steel bearings and a neoprene pad (see Figure 8). In addition to this, the girders over the piers were jacked up and the bearings greased. The objective was to get bearings at the abutments and on the piers that actually worked.

The first phase of testing was conducted between June 14th and 17th, 1999. The second phase occurred between July 26th and 29th, 1999 and the third phase on August 31st and September 1st, 1999.



Figure 7. Cut Separating Bridge Deck and Abutment



Figure 8. Original Bearings and Replacement Bearings

Static Testing

Bridge Diagnostics, Inc. (BDI) of Boulder, Colorado as a sub-contractor performed the static testing. BDI was responsible for executing the moving truck (crawl) load tests and for collecting and reducing the data for these tests. Researchers from Utah State University conducted the stationary truck load tests and all the dynamic testing.

Static Loading

Static loads were placed on the bridge using one or two 3-axle (10 wheel) dump trucks fully loaded with sand. The dimensions for these trucks and the loads each truck carried for the three test phases are shown in Figure 9. The time lag between tests conducted for each phase did not allow for the sand to be kept in the dump trucks. An effort was made to have consistent loads for each of the three test phases, and this was accomplished between phases 1 and 2, however, the loads used in phase 3 were lower by 20% for one truck and 13% for the other.

Two different types of static loads were placed on the bridge for all three test phases. The first type of load was semi-static or a crawl load, this consisted of creeping one or two of the 3-axle (10 wheel) dump trucks across the bridge on one of three prescribed routes (see Figure 10). The three prescribed routes for the trucks are shown in Figure 15 and noted as Y1, Y2 and Y3. The trucks traveled from south to north on these prescribed routes. When two trucks were used they were placed rear to rear and the forward truck towed the back truck across the bridge (see Figure 11). The second type of static load was truly static, it consisted of placing two dump trucks side by side but facing in opposite directions so that one of the rear axles for each truck would line up on the mid-span, inducing as large a deflection as possible at mid-span (see Figures 12, 13).

Instrumentation

Instrumentation for the static testing consisted of removable strain gages and string pot type linear voltage displacement transducers (LVDT's). The removable strain gages were used by BDI during the crawl tests to measure strain as the trucks moved across the bridge; this data was used to create the influence diagrams contained on the enclosed CD. The LVDT's were used to measure the mid-span displacements of each girder for the static truck loads.

BDI had 48 of the removable strain gages available to them for this project. This number of gages was a reasonable number for the instrumentation of one span, but not an entire bridge, so the instrumentation was done in three different set-ups. A total of 136 unique instrument locations were used for each test phase. Eight instrument positions were repeated between set ups one and three to verify reproducibility of the crawl tests. The first set-up was primarily an

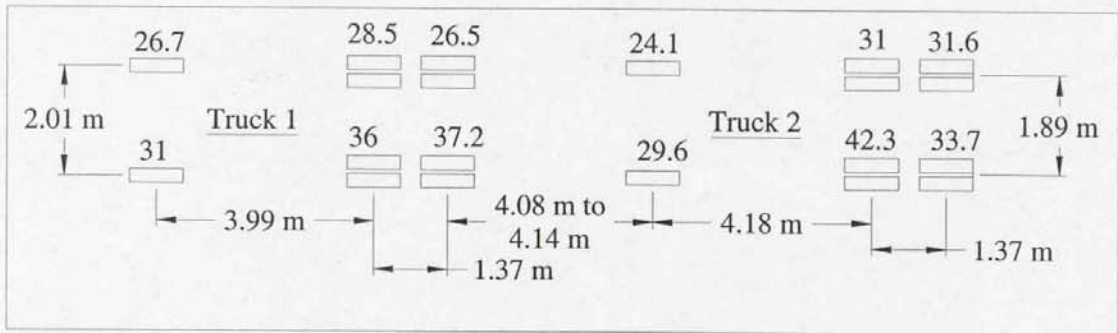
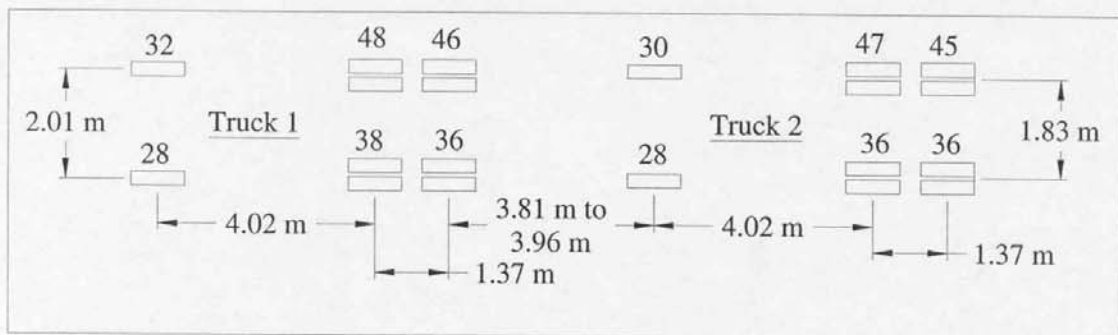
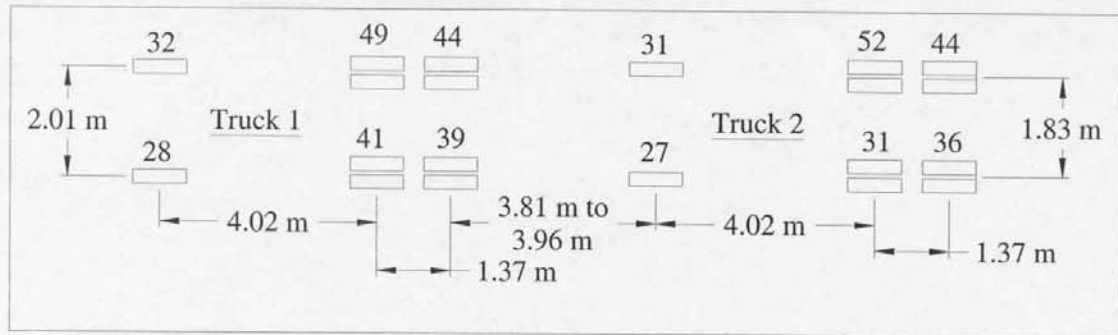


Figure 9. Truck Loads and Dimensions
(All loads in kilo-Newtons)



Figure 10. Single Truck Pass



Figure 11. Double Truck Pass

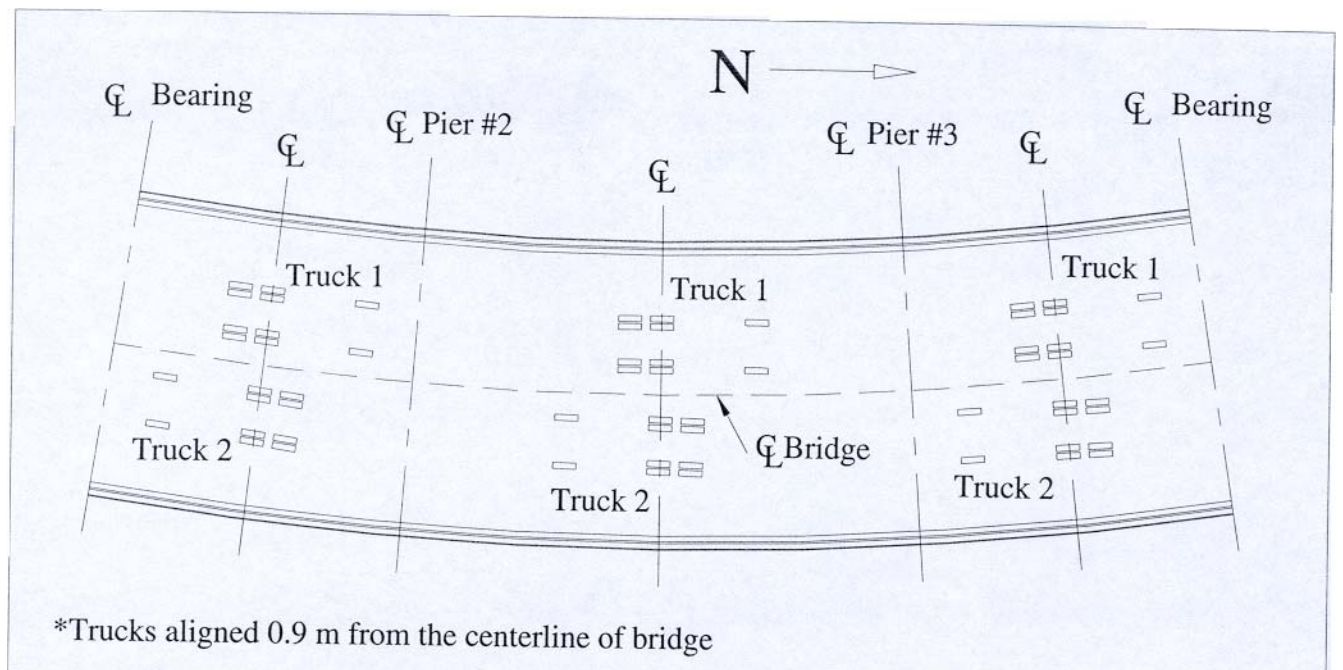


Figure 12. Truck Positions for Static Deflection Tests



Figure 13. Static Truck Load Position

instrumentation of the south span, the second set-up was for the north span and the third instrumentation set-up was mainly on the center span.

Typical gage locations on the girders and diaphragms are shown in Figure 14. All of the instrument locations for the entire bridge are shown in Figure 15, along with the truck paths. A single strain gage is shown on the underside of the top flange in Figure 6 and a typical strain gage array is shown in Figure 16.

The string pot LVDT's were used to measure mid-span displacements for the stationary truck loads. Five of these instruments were used, one for each of the support girders, and moved from span to span along with the strain gages.

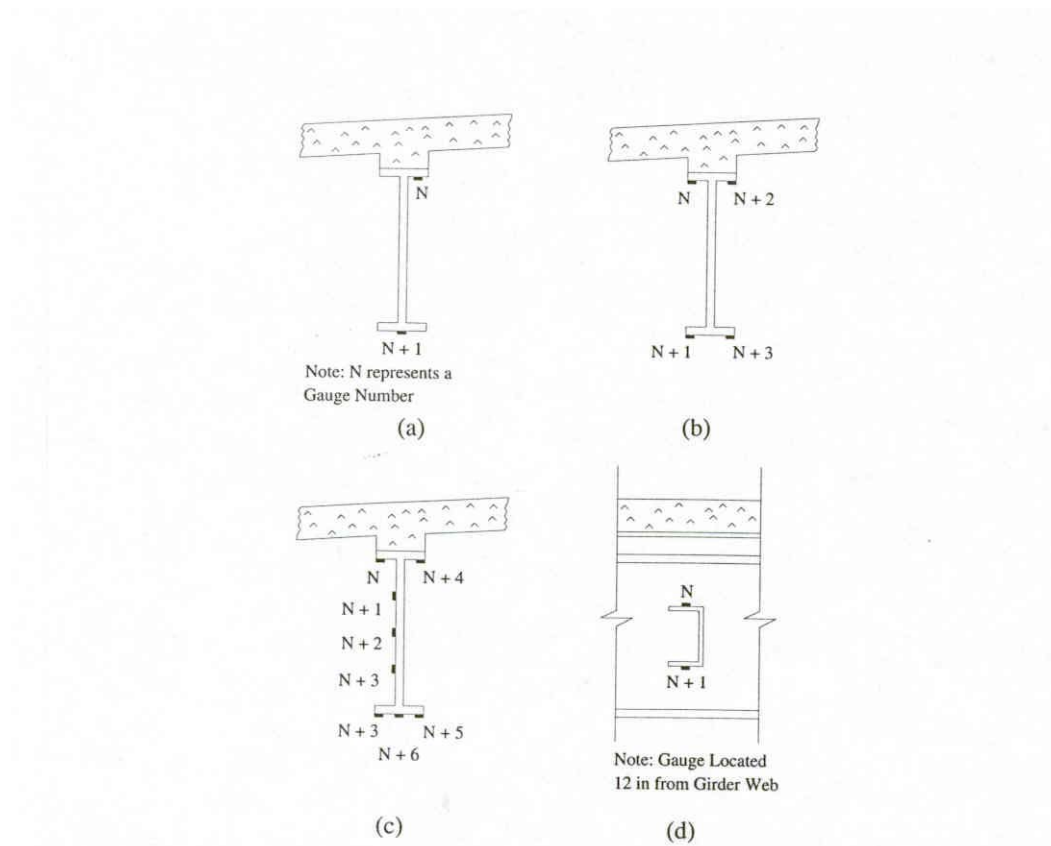


Figure 14. Typical Strain Gage Arrays

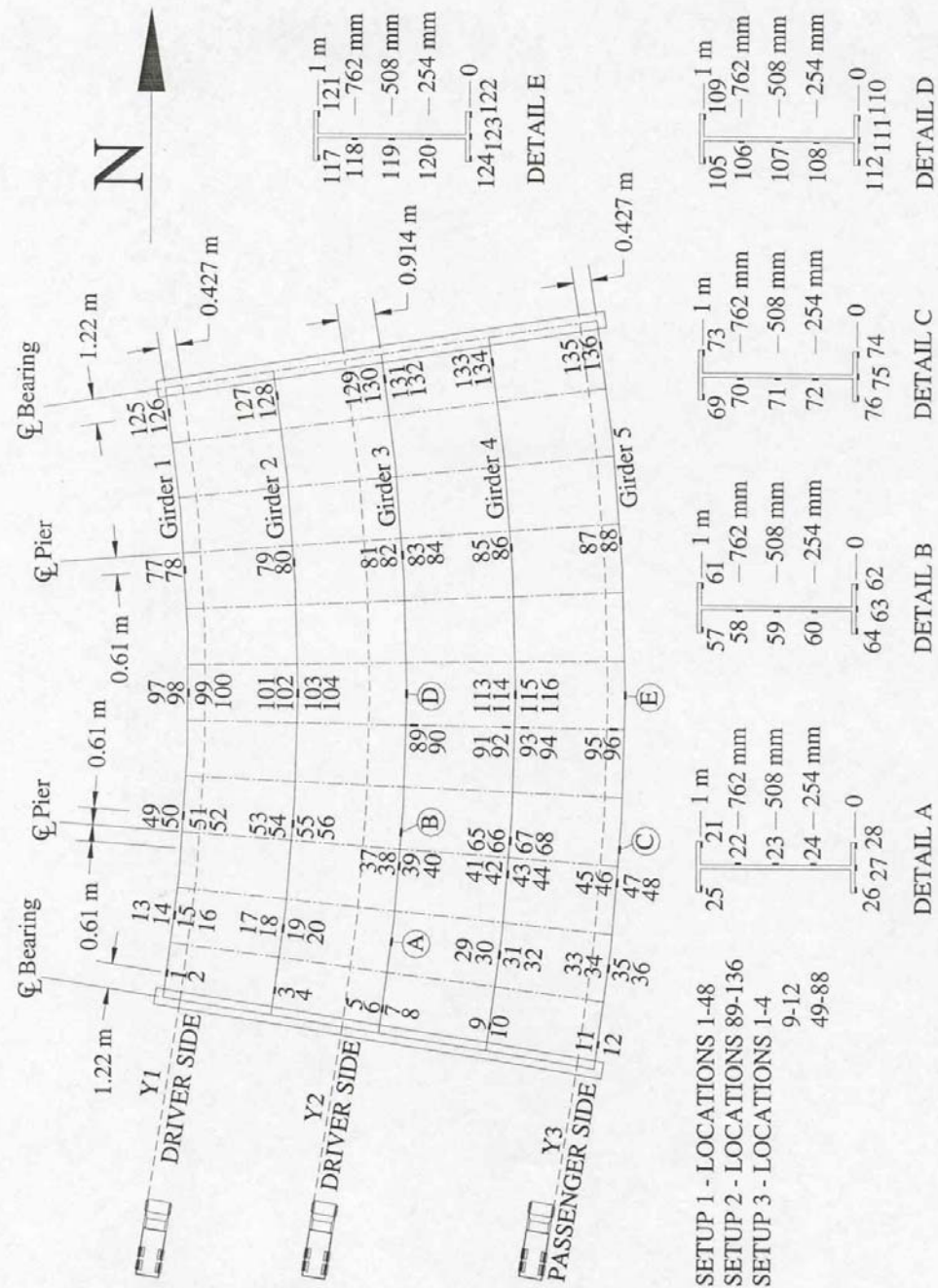


Figure 15. Strain Gage Placement and Truck Routes



Figure 16. Typical Strain Gage Array

The string pot LVDT's were used to measure mid-span displacements for the stationary truck loads. Five of these instruments were used, one for each of the support girders, and moved from span to span along with the strain gages.

Static Testing Procedure

The static testing with instruments set up on the outer spans was conducted during the day. Testing with instruments on the middle span was conducted at night, with the freeway below the bridge closed, allowing safe access to the girders in the middle span.

For strain measurements 30 truck passes were typically made over the bridge for each test phase. These truck passes consisted of running a single truck over each of the three truck routes (see Figure 15) twice and the double truck configuration over routes Y1 and Y2 twice also; this was done for each of the three instrumentation set-ups. The tandem truck load was not run over route Y3 because there was not enough room at the south end of the bridge to line the two trucks up in series.

Truck passes were made over the same route twice to ensure reproducibility of the test procedures and structural response. It also provided back-up data should something happen to the data of one pass.

The exception to the 30 truck passes occurred during the testing of the center span during the first phase where 28 truck passes were made. The double truck load was run over routes Y1 and Y2 only once for each route. This was the first time any tests had been conducted at night and time ran out (i.e. the freeway was opened) before all the truck passes could be completed.

After placing all the reusable strain gages on a particular span the truck passes were made. Guidelines for the three truck paths were painted on the asphalt deck surface. The movement of the truck was at a very low speed and the driver of the truck was assisted in following the prescribed route by a person standing on whichever running board of the truck lined up over the painted guidelines. It was noted that the drivers did very well in staying on the routes. The heavier truck of the two available was always used for the single truck load for each test phase, these trucks are denoted as Truck 1 in Figure 9. Truck 1 was also always the lead truck in the tandem configuration.

The strains measured by the gages and the position of the truck were all collected electronically, at a rate of 33.33 Hz, and stored on a computer. Strains were measured at all gages locations each time the truck progressed 64 mm (0.21 ft). The raw data was stored in ASCII text files. Converted data files were imported into Excel 97 spreadsheet files. For each test phase there are three spreadsheet files, one for each instrumentation set-up. Within the files are worksheets that represent each truck crossing, one worksheet per crossing. The first column of each of these worksheets is the truck position with respect to the south abutment, the rest of the columns contain data from the strain gages. It is these Excel 97 files that are used to produce the influence diagrams.

The deflection measurements for each girder at mid-span of each span were made using the string pot LVDT's with load provided by the side by side truck configuration (see Figure 12). With only five LVDT's on hand only one span was tested at a time and then the instruments were moved, just as with the strain gages. These truly were static tests, the trucks were brought to a stop and data recorded for two minutes. The main objective of this test was to get deflection data for the bridge, however, strains were also measured during these tests.

Dynamic Testing

The purpose of the dynamic testing is to investigate the potential for using dynamic testing, specifically modal analysis, as a non-destructive evaluation tool for the detection of structural damage. In Utah this damage would be most likely caused by an earthquake. The concept is based on the principle that natural frequencies and mode shapes are functions of structural stiffness and mass. Should a structure be damaged this would change the stiffness of the structure, but probably not the mass, and thereby alter the natural frequencies and mode shapes. If the dynamic characteristics of a structure are known before hand,

then after a potential damage causing incident the structure can be re-tested and dynamic characteristics compared to see if any damage has been inflicted on the structure. Changes (reduction) in natural frequencies will indicate damage and changes in mode shapes can indicate the location of damage. The key to this damage detection approach is to have tested a structure before a damage inducing event in order to know the undamaged structure's natural frequencies and mode shapes.

This bridge was not damaged, but the boundary conditions were altered twice to simulate damage. The bridge was tested dynamically in all three condition states, the same phases as in the static testing.

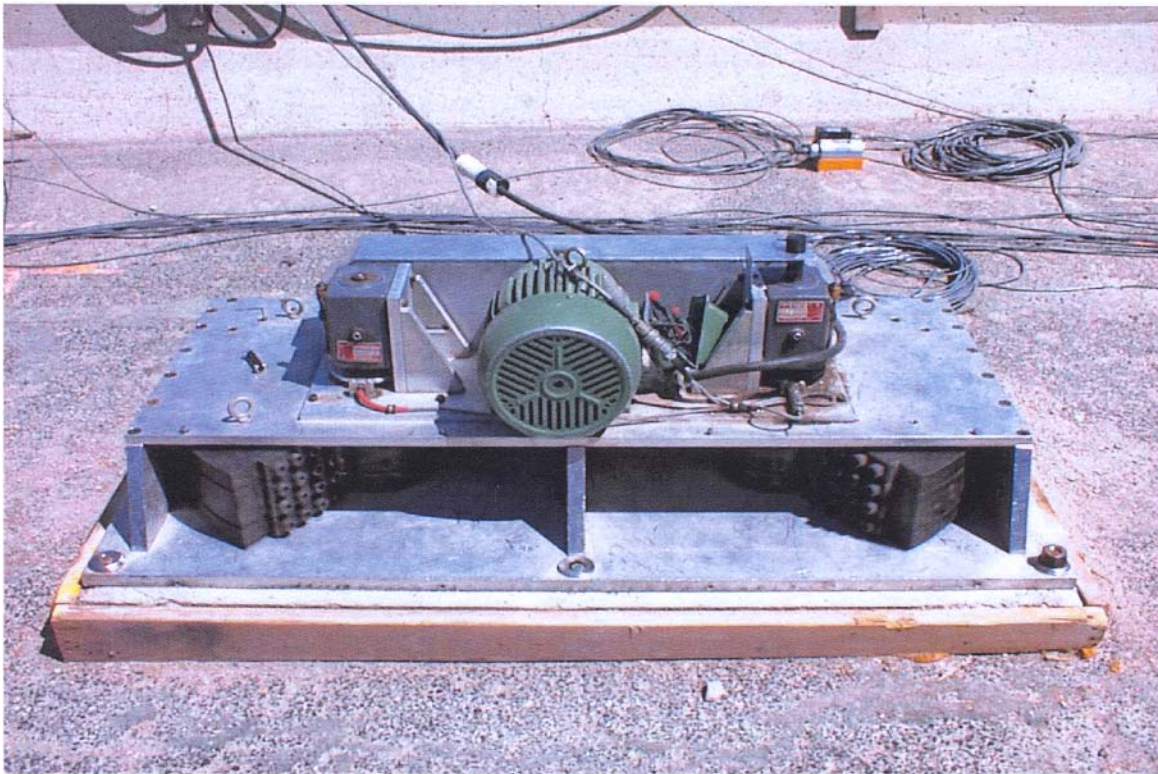


Figure 17. Eccentric Mass Shaker (looking East)

Dynamic Loading

The dynamic excitation of the bridge was accomplished using an eccentric mass shaker capable of providing a sinusoidal forcing function in any horizontal direction. The shaker utilizes weights that rotate in opposite directions about two spindles providing a force of up to 89 kN (20,000 lbf) at up to 20 Hz (see Figure 17).

The east edge of the shaker was placed 1.98 m (6Y2 ft) from the east parapet and the south edge was placed on the centerline of the south pier. This eccentric placement of the machine induced a torsional response of the bridge as

well as longitudinal and transverse responses. The shaker was not moved from that position for any of the three test phases.

Instrumentation

Forty-four velocity transducers (seismometers) and accelerometers were used to capture the response of the bridge to the dynamic excitation. Of these 44 instruments 21 were seismometers set up to record the horizontal motion of the bridge, the data from these instruments is what is the basis for the results outlined in this report. Figure 18 shows the placement of these seismometers and a typical array of instruments is shown in Figure 19, the cylindrical silver instruments are seismometers and the black box is an accelerometer.

The data from the instruments, along with the excitation force created by the shaker, were recorded on a personal computer using data acquisition software in combination with a 16-bit analog to digital converter card in series with anti-aliasing pre-filters.

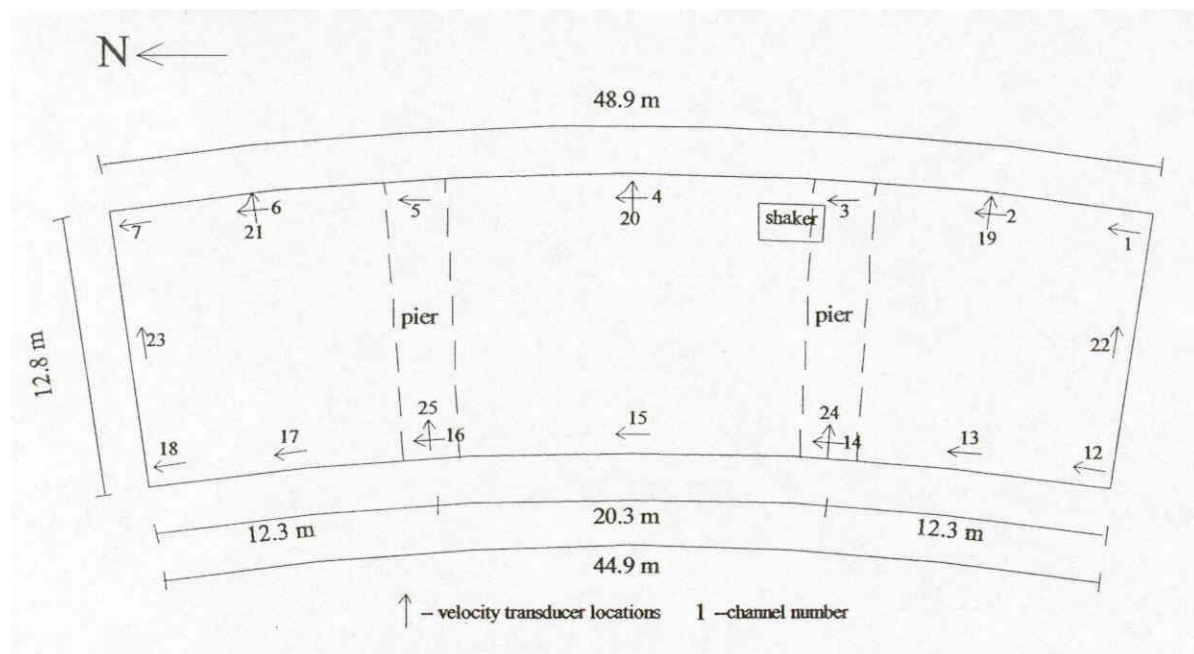


Figure 18. Placement of Seismometers on Bridge Deck

Dynamic Testing Procedure

After positioning and anchoring the mass shaker to the bridge, placing the instruments in their proper locations, and testing the data recording system, the mass shaker was run through a frequency sweep where the excitation frequencies of the shaker were increased from 0.5 Hz to 20 Hz in 0.02 Hz increments. Increasing the frequency of the machine was done automatically using a controller and the data acquisition computer. For excitation frequencies of 0.5 to 2 Hz the shaker would be run at a frequency for 41 seconds while

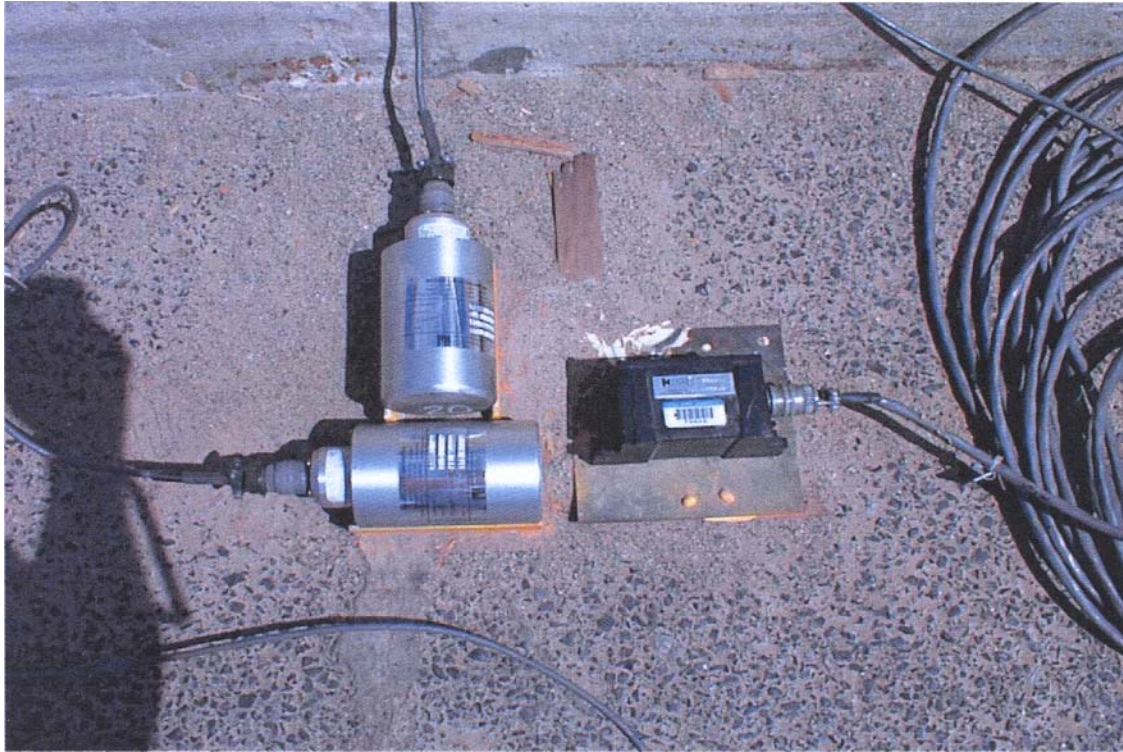


Figure 19. Typical Dynamic Instrumentation Array

response data was being recorded. At frequencies between 2 and 9 Hz the shaker would run at an excitation frequency for 21 seconds and for frequencies between 9 and 20 Hz the machine would run for 11 seconds. The sampling rate for response data in all cases was 100 Hz. After recording data for a given excitation frequency the shaker frequency was increased by 0.02 Hz and 6 seconds were then given for the bridge to settle into it's response at the new frequency. Then data was recorded at the new excitation frequency for the proper amount of time and the cycle repeated again until the excitation frequency reached 20 Hz. The process of going through this frequency sweep would take about eight hours.

For each condition state (i.e. test phase) the bridge was subjected to an excitation frequency sweep in both the transverse (radial) and longitudinal (tangential) directions.

Computer Model

A finite element model of the curved steel girder bridge was developed using SAP2000. This model will be used in future research investigating the types of analyses that need to be used to predict, in a sufficiently accurate manner, the behavior of curved girder bridges and, possibly, in the development of Load Resistance Factor Design (LRFD) equations for curved steel girders.

The model is a linear one using four node shell elements to model the girders, stiffeners, diaphragms and deck. Eight node block elements are used to model the parapet, which does add stiffness to the structure. The potential non-linear behavior between the deck and upper flange of the girders is modeled using two node beam elements that have a very high axial stiffness with a flexural stiffness that models the interface between the deck and girders and allows differential movement between the two surfaces.

The shell elements for the girder webs are square with two elements through the depth of the girder; the dimension on each side of these elements is approximately one-half the web depth of the girder, 0.41 m (16 in). The width of the flange elements is 0.41 m (16 in) to match the width of the web elements and the depth of the flange elements is one-half the flange width, 0.3 m (12 in). The web stiffeners are broken into two elements to match the web and flange elements.

Diaphragms are broken horizontally into seven elements, each element 0.38 m (15 in) wide. The webs of the diaphragms are just one element deep, as are the flanges.

The deck elements also have the same width as the girder web and flange elements; again, this is for compatibility. Transverse to the bridge deck there are five deck elements between each girder flange, which leaves a dimension of approximately 0.48 m (19 in) for each of these elements. The deck elements over the flanges are the same dimension as the girder flange elements.

The flexural elements used to model the interface between the deck and girders are placed at each node that is common to the girder flanges and the deck. This results in three elements spaced every 0.41 m (16 in) along the upper flange of each girder. The length of these elements is 0.13 m (5 in) or half the thickness of the bridge deck.

For the model of the bridge in the as-is condition the boundary nodes for the deck and parapets were fixed for all degrees of freedom. For the model of the second and third test phases these nodes were freed completely to simulate the cutting of the deck and parapets. The radial and vertical translations at lower flange nodes associated with the bronze rocker bearing supports were fixed for the first two test phases. Tangential movements at these nodes, and the nodes at the top flange of the girder, were also restricted by springs for the first two test phases in order to model the damaged bearing. The springs placed at the ends of the bottom flanges of the girders, in combination with the flexural link elements between the girders top flanges and the deck, provided the required rotational stiffness at the girder ends. The rotation about the radial axis at all nodes associated with bearing points was not restricted for any of the test phase models.

For the third test phase the girder end springs were removed at the abutment bearings and the position of the supports moved to node positions that correctly represent the new "frictionless" bearing and their proper positions (see Figure 8).

The total number of elements contained in this model is 11,387 for approximately 68,000 degrees of freedom.

To run this model for an analysis of the static loads used in the field to determine mid-span displacements takes 45 minutes on a 466 MHz personal computer. This analysis consists of only three load cases, the placement of the two trucks at the mid-point of each span, one span at a time.

The crawling truck load is simulated by moving static axle loads across the bridge at spacing increments of just more than 1.2 m (4 ft) on average. This analysis contains 230 total load cases for passing the single truck over all three routes and the double truck over routes Y1 and Y2. To run this analysis, which is how the computer model data was generated for the influence diagrams, takes three hours on the same 466 MHz personal computer.

Results

Crawl Load Tests

The repeatability of the crawl load tests was very good. The drivers did an excellent job of following the truck paths. Figure 20 shows the strains for a gage on the middle girder (girder 3) at the south pier (pier 1) for two separate double truck passes. This type of repeatability of bridge response data is typical.

The results for all of the crawl tests for all test phases are shown through influence diagrams contained on the enclosed CO. The CO is organized into three folders, one for each test phase. Within these folders are sub-folders for each truck route, Y1, Y2 or Y3. A "0" in the folder name indicates tandem truck runs over that route. The Excel files containing the influence diagrams are in these sub-folders. Each file name contains numbers which indicate which gages, or range of gages, the influence diagrams in that file were developed from.

Key results for each test phase are outlined in the following sections. Conclusions from these results are contained in the conclusion section which follows.

Phase 1 Tests

- The strain gages placed on the three interior girders at a distance of 1.22 m (4 ft) from the supports show the sign of the moment at this position on the girders to be the same as the sign of the mid-span moment (see Figure 21).

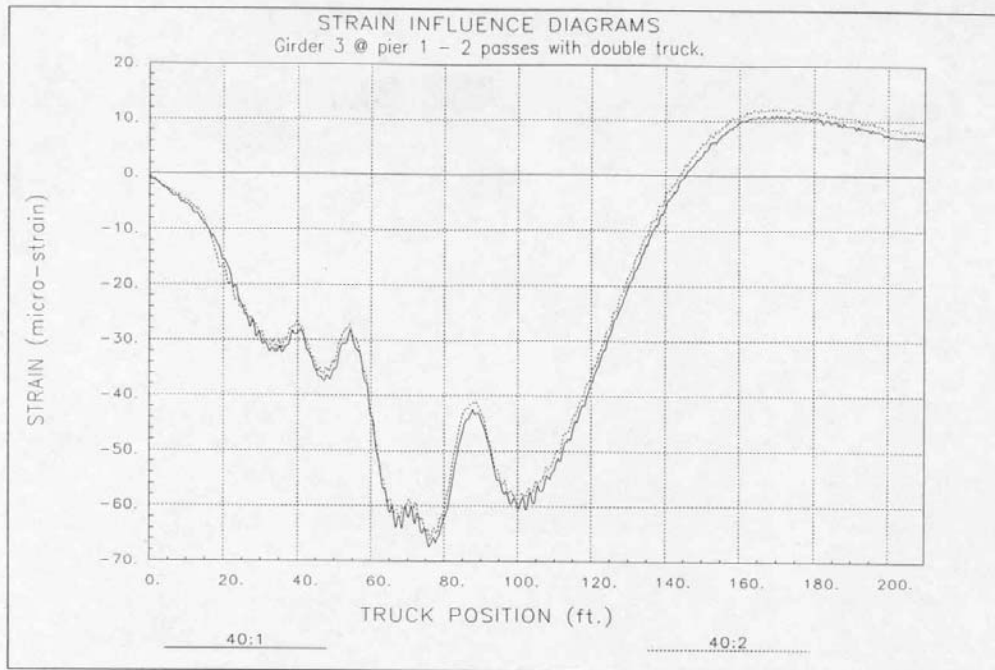


Figure 20. Repeatability of Data From Truck Passes (BDI)

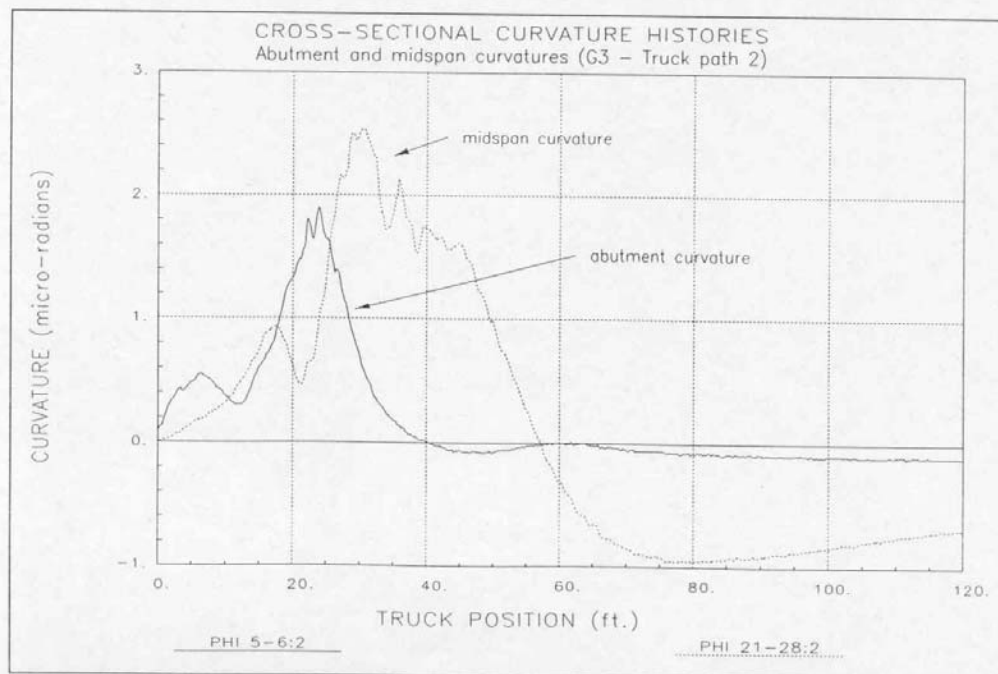


Figure 21. Abutment and Mid-Span Curvatures (BDI)

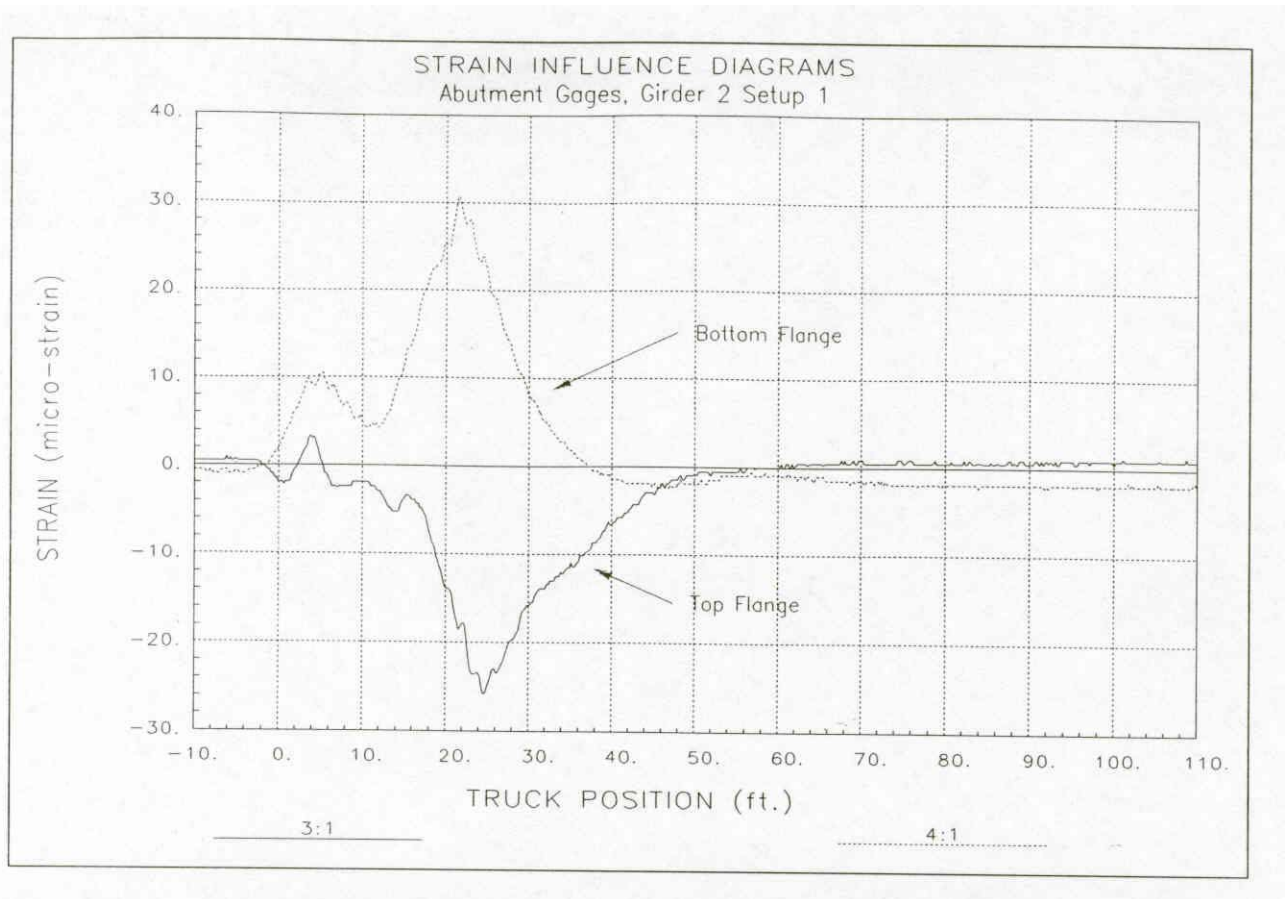


Figure 22. Typical Strains for Interior Girders at Abutments (BDI)

- The strains at this position on these girders are also close to the same magnitude for the upper and lower flanges (see Figure 22) indicating a moment of inertia provided by a symmetric cross section.
- After truck passes residual strains were evident in many gages. This residual strain was usually higher in the upper flanges than in the bottom flanges (see Figure 23).
- The strain gages on the exterior girders placed 1.22 m (4 ft) from the supports show the curvature (moment) of the beam at that point to be opposite that of the mid-span curvature (see Figure 24).
- Upper and lower flange gages placed at mid-span locations reveal upper flange strains at these locations to be much lower than those in the bottom flange (see Figure 25).

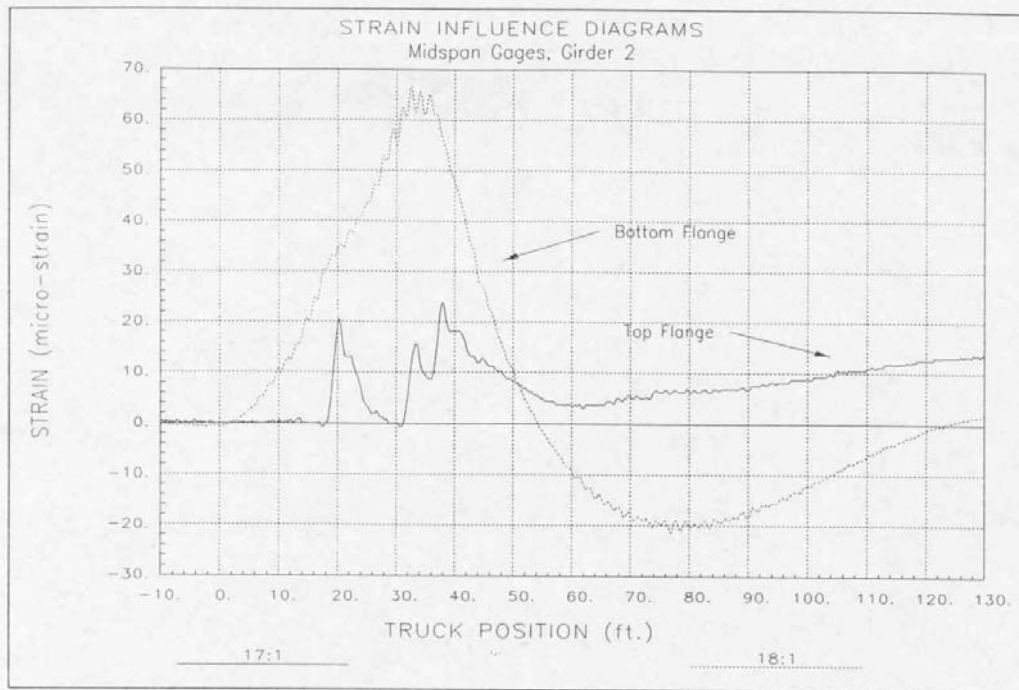


Figure 23. Typical Residual Strain in Girders (BDI)

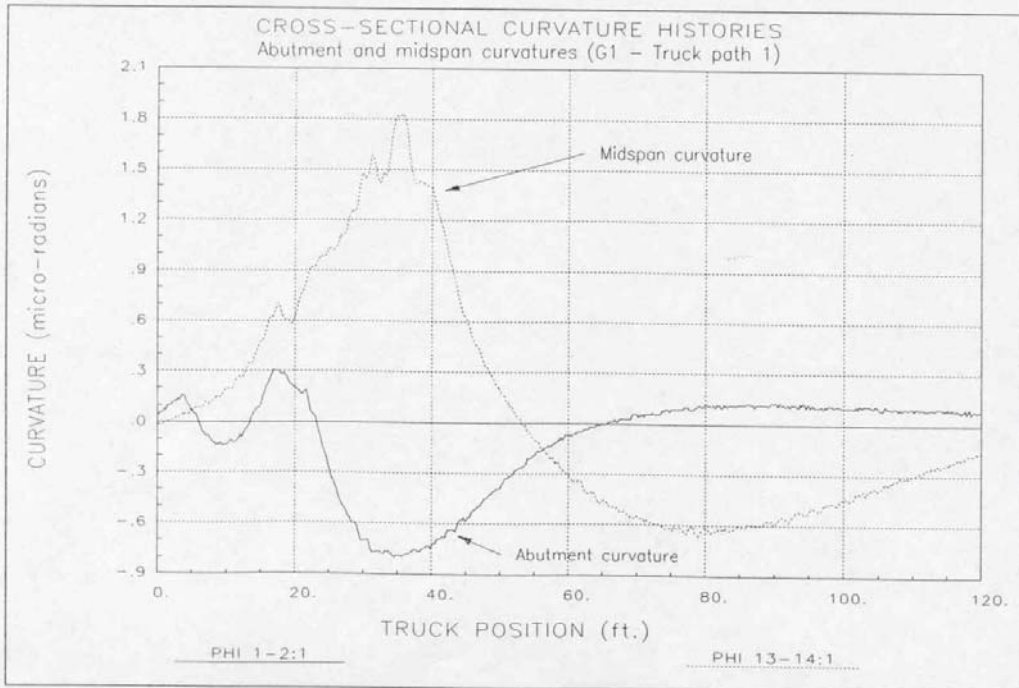


Figure 24. Girder Curvature at Abutment and Mid-Span (BDI)

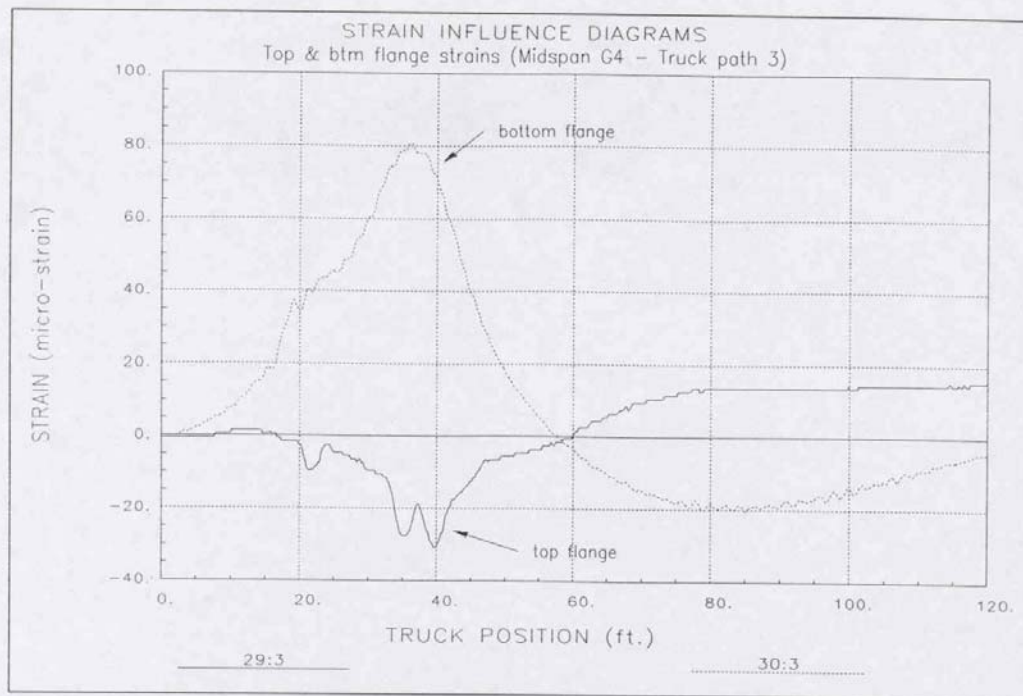


Figure 25. Typical Upper and Lower Flange Strains at Mid-Span (BDI)

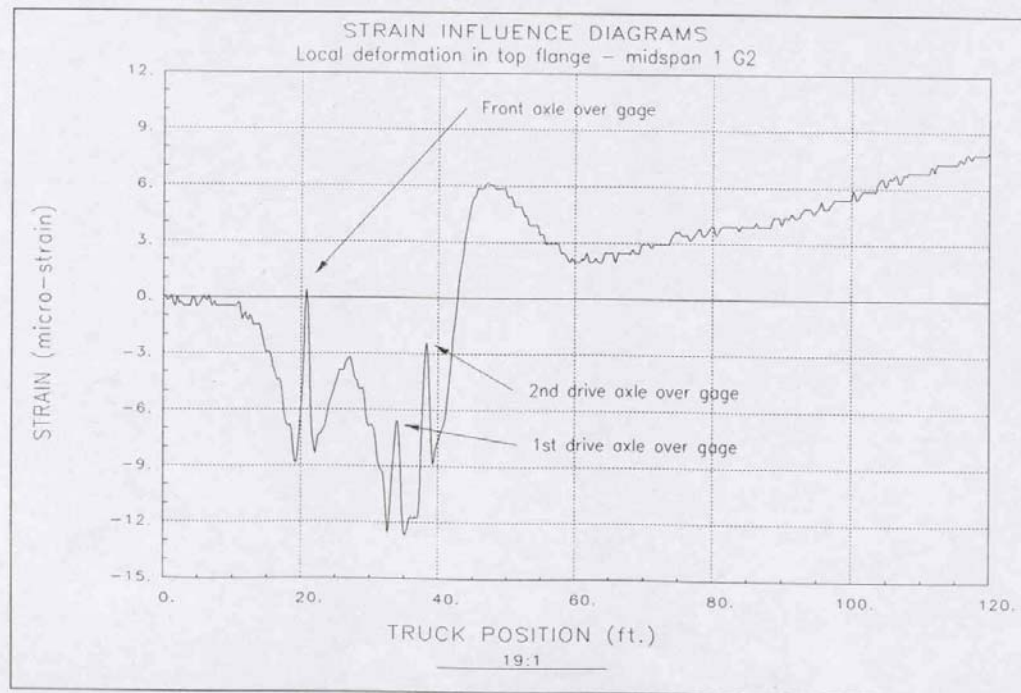


Figure 26. Tension Spikes in Girder Upper Flange (BDI)

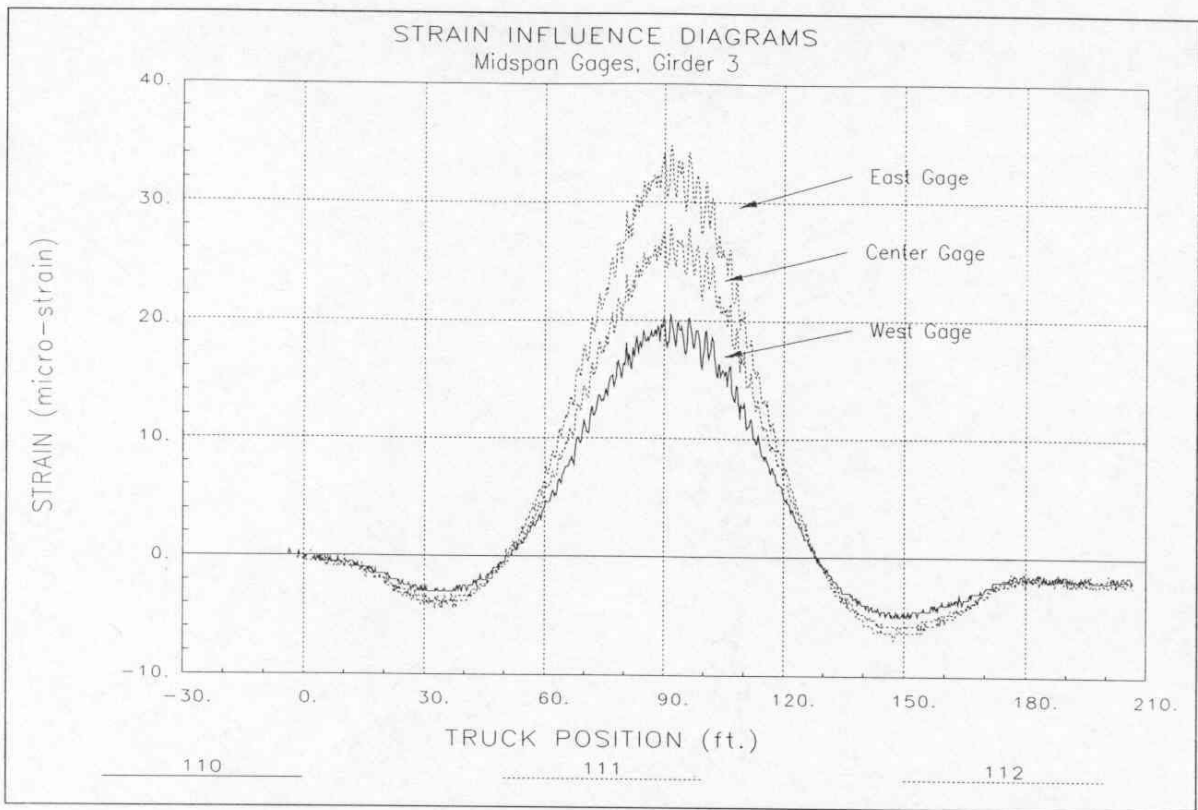


Figure 27. Transverse Strain Variation in Lower Flange of Girder (BDI)

- Upper flanges of girders experience tension spikes in the influence diagrams as shown in Figure 26. These tension spikes indicate local deformations of the flange.
- Transverse strain distribution across the bottom flanges of the girders indicates significant lateral bending (see Figure 27).

Phase 2 Tests

- The strains in the bottom flanges of the exterior girders increased significantly with the cutting of the deck and approach those values experienced by the interior girders in phase 1 tests, this is seen in Figure 28 and in a comparison with Figure 22.
- The magnitudes of moments at the mid-spans of the end spans increased slightly, from zero to 10 percent.

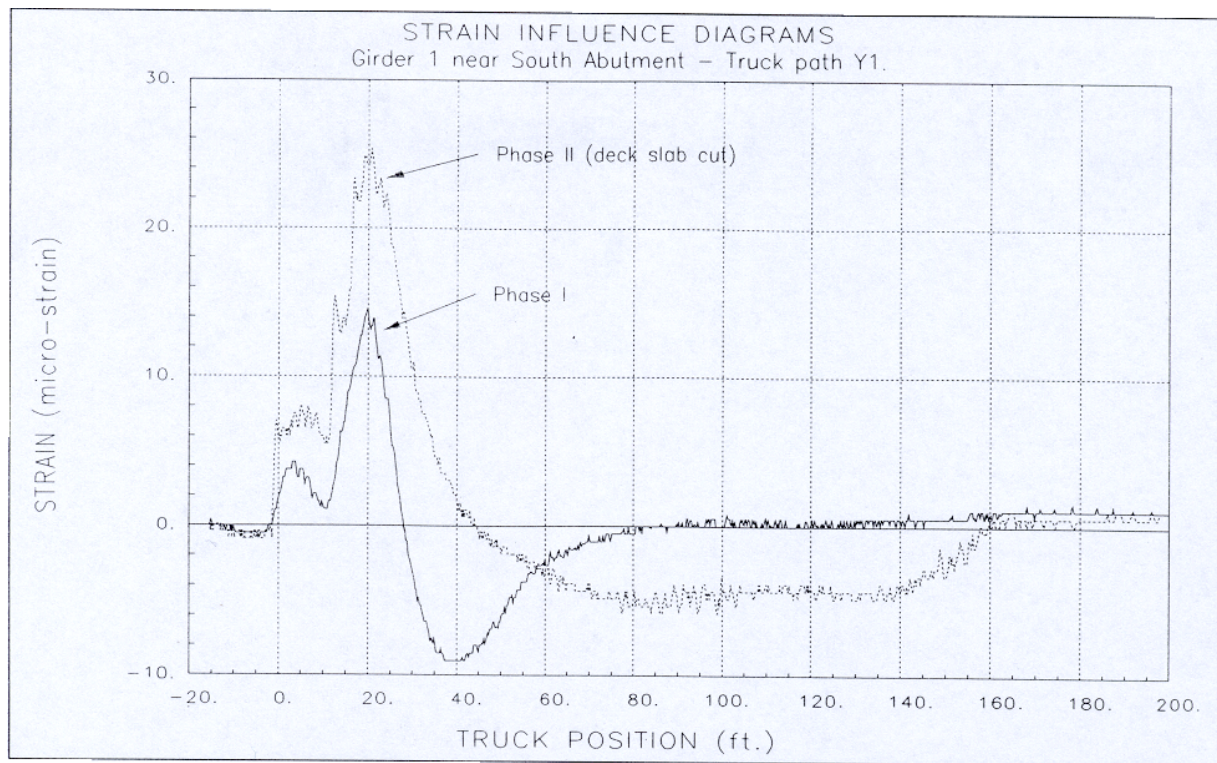


Figure 28. Strain Comparison Between Phase 1 and Phase 2 (BDI)

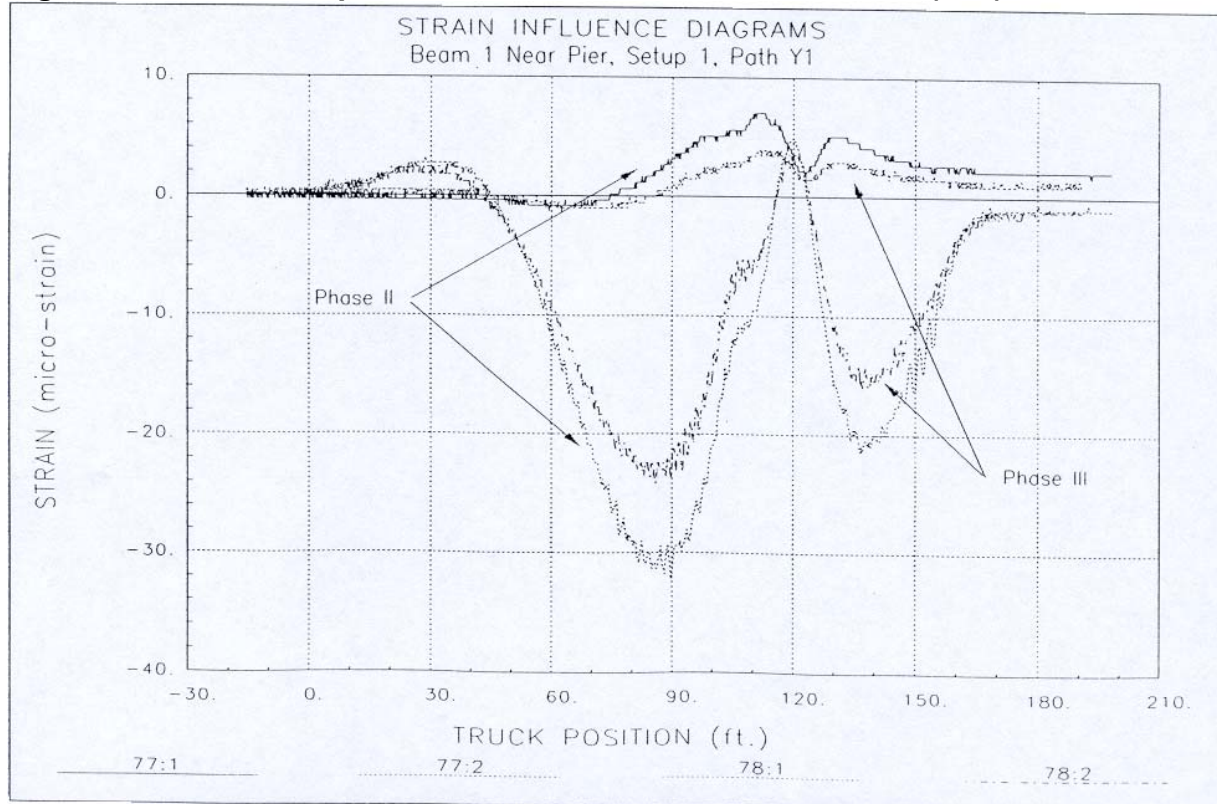


Figure 29. Strain Comparison Between Phase 2 and Phase 3 (BDI)

Phase 3 Tests

- Qualitatively, the response of the bridge during phase 3 tests is very similar to that of phase 2 tests (see Figure 29). Quantitative comparisons are difficult due to the significantly lower truck weights used in the phase 3 tests.

Static Load Tests

The results of the static load tests are shown in Table 2. This data was collected primarily to use as a way to verify the computer model that has been developed.

Computer Model

The deflections at the centerline of each span as calculated by the computer model are compared to the field deflection measurements in Table 2. The percentage error in the calculation of these deflections by the computer model is shown in Table 3. The model is most accurate in determining deflections in the girders that are directly under the load, with percentage error less than 10 percent.

The higher percentage error occurs in the deflection calculations for the girders that are farthest from the load; this error exceeds 300 percent in one case but is typically between 100 and 200 percent. However, these percentage numbers can be misleading. Deflections at the centerlines of the girders farthest from a given load path are on the order of hundredths of a millimeter, so the slightest variation between the model and the field data results in large percentage differences. When the actual deflections are larger, the computer model results are much closer to the field data and the percentage error much smaller.

Influence diagrams for girder strains calculated by the computer model are superimposed on influence diagrams for the actual field strain. From a qualitative point of view the influence diagrams developed from the computer compare well with the test results. The strains in the bottom flanges of the girders as calculated by the model are very close to the actual strains; with the results being better when a girder has the load placed directly over it.

The main discrepancy between the computer model strains and the field data occurs on the top flanges of the girders at the centers of the spans. Despite the fact that the bridge is non-composite in nature at the centers of each span the girders and the deck behave in a very composite manner. The field data shows the neutral axis to be in the deck of the bridge at these points causing the top flange to be in tension. The computer model consistently shows the strains in these regions to be compressive, as it would be in a non-composite bridge. Varying the flexural stiffness of the link elements between the girders and the

deck as one moves along a span, with larger stiffnesses at the centers of the spans, could improve the results of the computer model in these instances.

Dynamic Testing

The changes in natural frequencies for this bridge as the boundary conditions were altered, as determined by the modal analysis, are shown in Table 3. Each change in boundary conditions resulted, generally, in a reduction of the natural frequencies for each condition state.

The exception to this is the natural frequency associated with the second mode shape. In the undamaged condition all of the modes determined by the dynamic excitation were similar in shape to the fundamental transverse mode. This is due to the fixity of the boundary conditions at the ends of the bridge. The second condition state, with the deck cut away from the approach slab and abutment, allowed much more movement at the ends of the bridge. All the mode shapes indicated this change in the boundary conditions. The fundamental mode shape remained basically the same with a drop in frequency, as was expected. The second mode, however, is completely different going from a variant of the fundamental mode to a mode shape that is as a second mode should be, with a node at the center of the bridge, as shown in Figure 30. This is a case where an alteration in a structure could not be determined by relying solely on the change in natural frequencies but required the use of the mode shapes to show exactly what happened to the structure.

An unexpected trial for using mode shapes to determine damage locations occurred prior to the testing of the bridge in the third condition state. When the intermediate support bearings were freed (and greased) and the end bearings placed on frictionless bearings this allowed the bridge to shift to the north (in the downhill direction). The result of this shift was a single contact point about 18 inches wide between the bridge deck and the north approach slab. When the mode shapes were analyzed for the dynamic testing in the third condition state this point showed up very clearly as a point of rotation for the first mode, showing the contact between the deck and the abutment. This is the best evidence yet that mode shapes can be used to determine the locations of significant structural changes or damage.

SPAN LOADED	SPAN MEASURED	GIRDER NUMBER									
		Girder Deflections (mm)									
		Model 1	Field 1	Model 2	Field 2	Model 3	Field 3	Model 4	Field 4	Model 5	Field 5
Phase 1 Tests											
1	1	-0.65	-0.65	-2.28	-2.37	-2.52	-2.41	-1.93	-1.97	-0.56	-0.58
1	2	0.31	0.27	0.56	0.55	0.66	0.69	0.54	0.50	0.30	0.23
1	3	-0.04	-0.02	-0.07	-0.07	-0.07	-0.08	-0.07	-0.05	-0.05	-0.09
2	1	0.31	0.13	0.62	0.37	0.73	0.72	0.59	0.65	0.33	0.20
2	2	-1.64	-1.63	-4.24	-4.22	-5.16	-5.16	-4.19	-4.23	-1.80	-1.71
2	3	0.31	0.23	0.60	0.56	0.73	0.73	0.62	0.57	0.38	0.09
3	1	-0.04	-0.11	-0.07	-0.19	-0.07	0.01	-0.06	0.14	-0.05	0.03
3	2	0.29	0.31	0.54	0.58	0.66	0.69	0.56	0.50	0.34	0.29
3	3	-0.56	-0.57	-2.09	-2.11	-2.55	-2.52	-2.10	-2.11	-0.71	-0.73
Phase 2 Tests											
1	1	-0.69	-0.61	-2.54	-2.37	-2.96	-2.76	-2.20	-2.37	-0.61	-0.69
1	2	0.35	0.19	0.63	0.51	0.75	0.59	0.61	0.38	0.64	0.15
1	3	-0.05	0.00	-0.08	-0.04	-0.09	-0.02	-0.08	-0.04	-0.06	-0.06
2	1	0.36	0.13	0.70	0.44	0.82	0.56	0.66	0.36	0.38	0.15
2	2	-1.63	-1.68	-4.26	-4.24	-5.32	-5.27	-4.27	-4.19	-1.80	-1.66
2	3	0.35	0.24	0.67	0.62	0.82	0.82	0.69	0.56	0.44	0.17
3	1	-0.05	-0.02	-0.09	-0.11	-0.09	-0.13	-0.08	-0.11	-0.06	-0.06
3	2	0.32	0.12	0.61	0.38	0.75	0.46	0.63	0.27	0.38	0.05
3	3	-0.60	-0.54	-2.35	-2.10	-3.01	-2.58	-2.39	-2.22	-0.77	-0.67
Phase 3 Tests											
1	1	-0.59	-0.44	-1.99	-1.64	-2.23	-2.22	-1.76	-2.04	-0.52	-0.49
1	2	0.28	0.14	0.49	0.37	0.58	0.47	0.48	0.33	0.27	0.13
1	3	-0.03	-0.07	-0.05	-0.11	-0.06	-0.10	-0.05	-0.07	-0.03	-0.05
2	1	0.28	0.11	0.54	0.49	0.64	0.77	0.53	0.60	0.32	0.20
2	2	-1.38	-1.33	-3.54	-3.46	-4.18	-4.61	-3.54	-3.93	-1.60	-1.64
2	3	0.28	0.12	0.53	0.37	0.65	0.50	0.55	0.38	0.35	0.12
3	1	-0.03	-0.06	-0.05	-0.02	-0.06	0.10	-0.05	0.09	-0.03	-0.02
3	2	0.25	0.22	0.47	0.36	0.57	0.41	0.50	0.27	0.32	0.10
3	3	-0.51	-0.60	-1.81	-1.71	-2.20	-2.23	-1.92	-2.05	-0.70	-0.73

Table 2. Deflection Data for Computer Model and Field Tests

Percent error due to load in span 1 (mm)					
	Girder 1	Girder 2	Girder 3	Girder 4	Girder 5
Span 1	0	4	-4	2	4
Span 2	-13	-2	5	-7	-23
Span 3	-50	0	14	-29	80
Percent error due to load in span 2 (mm)					
	Girder 1	Girder 2	Girder 3	Girder 4	Girder 5
Span 1	-58	-40	-1	10	-39
Span 2	-1	0	0	1	-5
Span 3	-26	-7	0	-8	-76
Percent error due to load in span 3 (mm)					
	Girder 1	Girder 2	Girder 3	Girder 4	Girder 5
Span 1	175	171	-114	-333	-160
Span 2	7	7	5	-11	-15
Span 3	2	1	-1	0	3

Table 3. Percent Displacement Error, Model vs. Field Data

	Condition 1 (undamaged)	Condition 2 (boundary change 1)	Condition 3 (boundary change 2)
Mode 1	5.33 Hz	3.84 Hz	2.89 Hz
Mode 2	5.85 Hz	6.05 Hz	5.29 Hz
Mode 3	7.44 Hz	6.66 Hz	5.63 Hz
Mode 4	8.63 Hz	8.48 Hz	6.32 Hz
Mode 5	12.12 Hz	11.60 Hz	8.46 Hz

Table 4. Changes in Natural Frequencies for Bridge

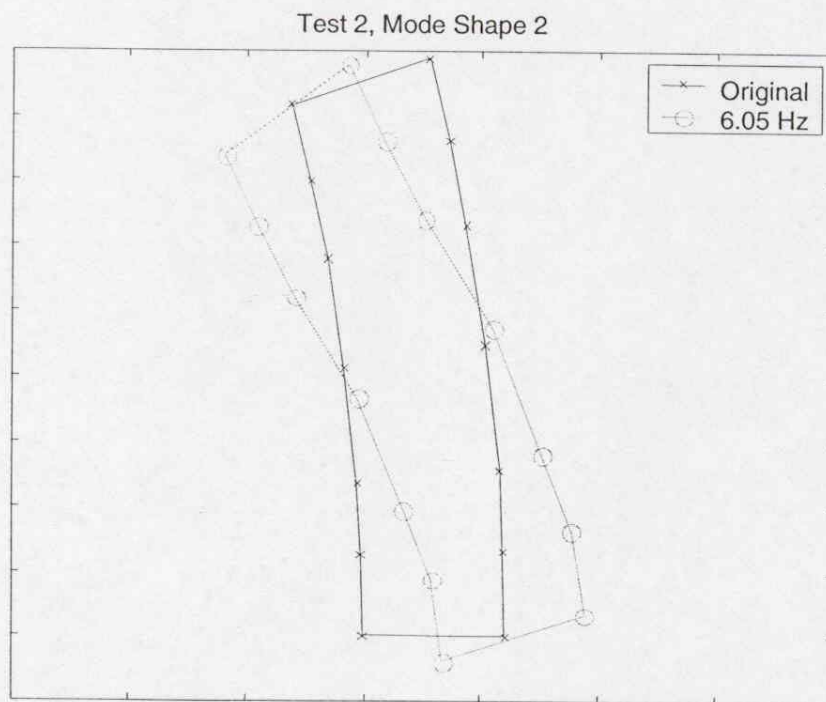
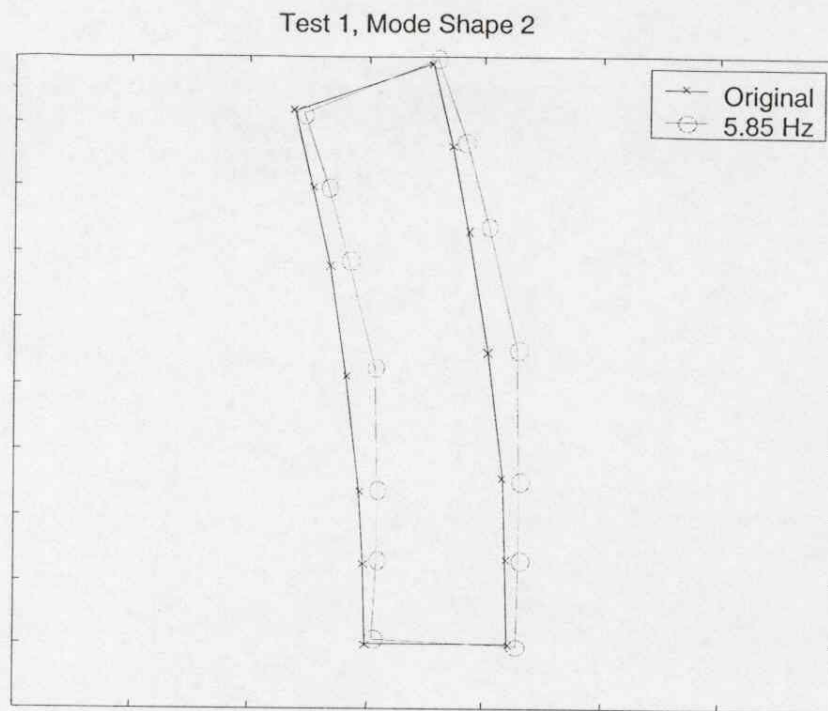


Figure 30. Changes in Mode Shapes for Bridge

Conclusions

Static Testing

Based on a review of the influence diagrams and the notes made in the Results section of this report several conclusions can be made with respect to the behavior of this curved steel girder bridge:

- The boundary conditions at the abutments for the three interior girders acted as pinned supports. The continuous deck had little effect on the behavior of these girders at the supports.
- The evidence of higher residual strain in the upper flanges compared to the lower flanges, and the behavior of the interior girders at the supports, leads to the conclusion that at the abutments the interior girders and deck behaved in a non-composite fashion. The non-linear form of the influence diagrams also indicates non-composite behavior.
- The boundary conditions at the abutments for the two exterior girders acted more as fixed supports than pinned. The stiffness added by the continuous parapet may have contributed to this behavior.
- The girders and deck behaved in more of a composite manner at the centerline of each span. This is indicated by the tensile strain in both the upper flanges and lower flanges of each girder.
- Upper flanges of the girders experience significant local deformations due to wheel loads.
- Significant lateral bending occurs in the girders and is demonstrated by varying strain across the lower flanges in the transverse direction. This is due to a combination of the super-elevation and the curve in the girders. The role each of these factors plays in the amount of lateral bending should be investigated further.
- The cutting of the deck induced more of a pin support behavior in the exterior girders.
- A computer model has been developed that predicts the maximum mid-span deflections of the curved girder bridge to an error of five percent or less.
- The same computer model predicted maximum tensile bending strains in the lower flanges of the bridge girders to within 20 percent accuracy.

- Based on computer analyses, removing the diaphragms resulted in an increase in stress of up to nine percent on the bottom flanges of the bridge girders.
- As the diaphragms were removed in the model, the location of the maximum bending stresses changed from the inside lower flange of girder 1 to the inside bottom flange of girder 3. This shift is from the exterior of the bridge to the center girder .

Some influence diagrams were not drawn for certain gage locations under certain loading conditions. This is because the strains indicated by these gages in those cases were no larger in magnitude than the noise in the data collection system. The gages not used did not vary by test phase, but did by load path. The following is a list by route, and type of truck load, of gages for which influence diagrams were not drawn:

Y1 and DY1	gages 9-11, 33-36, 45-48, 65-76, 87-88, 133-136.
Y2 and DY2	gages 1-2, 11-12, 125-126, 135-136.
Y3	gages 1-4, 49-56, 77- 78, 125-126.

Comparing these gage numbers with their positions as given in Figure 15 shows that for truck loads passing over route Y1 there was very little strain picked up in the girder farthest from that load path, girder 5. The reverse of that is also true, with very little strain in girder 1 for loads over route Y3, especially since Y3 had only single truck loads. As for loads run over path Y2, the gages near the abutments of girders 1 and 5 experienced little strain, due to the stiffness of the boundary conditions there and the distance of the girders from the load.

It should be noted that all of the diaphragm gages were used for all load cases to develop influence diagrams. This would indicate that the diaphragms were transferring lateral loads.

Computer Model

Comparing the results of the field tests to the results of the computer model analyses shows that a linear finite element model of this bridge has been developed that replicates reasonably well the non-linear behavior of the actual bridge. Additional modifications could be made in the linear model to improve its performance, allowing for varying stiffnesses in the link elements between the girders and deck being perhaps the best modification that could be made, however, it is still a linear model attempting to model very complicated non-linear behavior .

The computer model, with some modifications (improvements) will be used in the next phase of this research to examine the effect of the super-

elevation, by flattening out the model, in addition to the level of analysis study that will be performed.

Dynamic Testing

The dynamic testing performed on this bridge support the premise that modal analysis can be used as a non-destructive evaluation technique for determining the location and type of damage a structure has experienced due to a catastrophic event. The changes in the natural frequencies of this structure presented in this report are related to changes in the stiffness of the structure due to the alterations in the bridge's boundary conditions. In addition, the changes in the modes shapes as a result of changing the boundary conditions are consistent with the types of alterations made in the boundary conditions and provided information as to the location of the changes made in the stiffness of the structure.